Model-Based Multiscale Detection of 3D Vessels

Karl KRISSIAN, Grégoire MALANDAIN, Nicholas AYACHE
Epidaure project INRIA - 2004, route des Lucioles
06902 Sophia Antipolis France
emails: {kkrissia,greg,na}@sophia.inria.fr

Régis VAILLANT, Yves TROUSSET
General Electric Medical Systems BP 34
78533 Buc Cedex, France
emails: {vaillre,trousyv}@gemse.fr

Abstract

In this paper, we present a new approach to segment vessels from 3D angiography of the brain. Our approach is based on a vessel model and uses a multiscale analysis in order to extract the vessel network surrounding an aneurysm. Our model allows us to choose a criterion based on the eigenvalues of the Hessian matrix for selecting a subset of interesting points near the vessel center. It also allows us to choose a good parameter for a γ-normalization of the single scale response. The response at one scale is obtained by integrating along a circle the first derivative of the intensity in the radial direction. Once the multiscale response is obtained, we create a smoothed skeleton of the vessels combined with a MIP or a volume rendering to enhance their visualization. The method has been tested on a large variety of 3-D images of the brain, with excellent results. Vessels of various size and contrast are detected with a remarkable robustness, and most junctions are preserved.

1 Introduction

The purpose of this work is to detect the vessel structures in 3D angiographies of the brain in order to help the interpretation of the vessel network, especially in the vicinity of aneurysms. Our work is based on previous works already done by Koller et al [KGSD95], Lorenz et al [LCBF97], Furst et al [FKMP97], Lindeberg [Lin96, Lin94]. It is also closed to the work of [SNAK97]. We will successively present the acquisition process, related approaches, our method, results and conclusion.

2 Image Acquisition

The images were produced by General Electric Medical Systems Europe (GEMSE). They are obtained by 3D reconstruction of the vessels from 2D X-ray substracted angiographies. Details of the reconstruction scheme can be found in [Pay96]. Compared to the other 3D acquisition modalities which are Magnetic Resonance Angiography and Scanner Angiography, this 3D reconstruction gives a high isotropic resolution over the whole reconstructed volume. Nevertheless, it requires a good opacification of the vascular network obtained with an intra-arterial injection. Some MIPs of the given images centered on an aneurysm are shown in Fig 1. The images we are

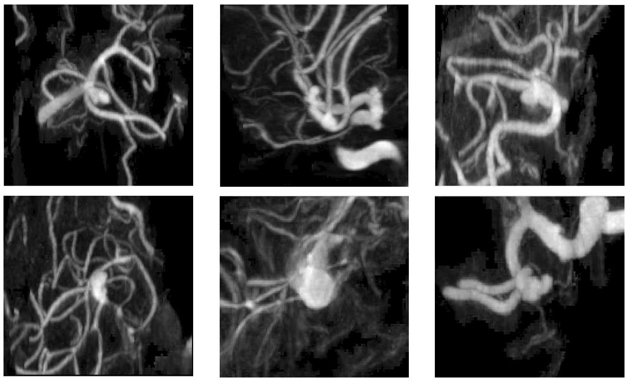

Figure 1: Maximum Intensity Projection of 6 different 3D images (images are $128 \times 128 \times 128$).

dealing with contain different artefacts: noise, partial volume effect, consequences of the patient motion between different acquisitions and 3D reconstruction artefacts which lead to a non-homogeneity of the intensity of the vessels for different vessel sizes (Fig 2 shows three isosurfaces of the initial image; small vessels are only visible with a low threshold).

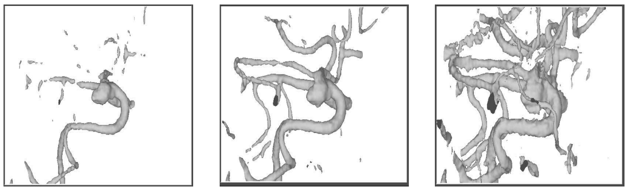

threshold 2200 threshold 1600 threshold 1000

Figure 2: Isosurfaces of the third image with different thresholds.

3 Multiscale extraction of vessels

The general approach of multiscale methods is to choose a range of scales and to compute a response for each scale from the initial image. All the responses are then combined to get a single multiscale response which contains the sought features. The general fundations of the scale-space theory can be found in [Lin94]. More formally, for a fixed scale s, we calculate a response image at that scale $R_s(I)$ where I is the initial image. Then we calculate the multi-scale response for the image $R_{multi}(I)$ which is for each point the maximum of the responses over scale:
for each point $x \in I$ and a range $[s_l, s_h]$ of scale,

$$R_{multi}(x) = \max_s \{R_s(x), s \in [s_l, s_h]\}. \quad (1)$$

This response $R_{multi}(x)$ can be interpreted as an indicator that the point x belongs to the center line of a vessel, and $R_s(x)$ can be interpreted as an indicator that the point x belongs to the center line of a vessel with radius s.
In [KGSD95], $R_s(I)$ is taken as the minimum among the 4 points $(x_i \in \{x \pm s\overrightarrow{v_1}, x \pm s\overrightarrow{v_2}\})$ of the absolute value of the first derivative of the intensity at x_i in the direction of $\overrightarrow{xx_i}$.

$$R_s(x) = \min\{\, |\nabla I_s(x + s\overrightarrow{v}).\overrightarrow{v}|\,, \overrightarrow{v} \in \{\pm\overrightarrow{v_1}, \pm\overrightarrow{v_2}\}\} \quad (2)$$

where $I_s = I * G_s$ is the image convolved with a

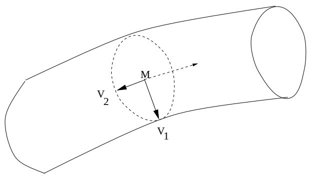

Gaussian G_s with standard deviation s, for $\overline{x} \in \mathbb{R}^n$

$$G_s(\overline{x}) = G_\sigma(\overline{x}) = \frac{1}{\left(\sqrt{2\pi}\sigma\right)^n} e^{\frac{-<\overline{x},\overline{x}>}{2\sigma^2}}$$

and $(\overrightarrow{v_1}, \overrightarrow{v_2})$ is a basis of unitary vectors in the plane orthogonal to the axis of the vessel. The vectors $\overrightarrow{v_1}$ and $\overrightarrow{v_2}$ are obtained from the eigenvectors of the Hessian matrix H^* of the image at a given scale $s = \sigma$: $H^*(x) = H_\sigma(x) = H(I * G_\sigma)(x)$. We note $\lambda_1, \lambda_2, \lambda_3$ the eigenvalues of H^* and $\overrightarrow{v_1}, \overrightarrow{v_2}, \overrightarrow{v_3}$ the associated unitary eigenvectors; with $|\lambda_1| \geq |\lambda_2| \geq |\lambda_3|$. [LCBF97] distinguish four cases depending on the structure (line or plane) and on its intensity (bright or dark). In the case of a bright structure with a dark background,

$$\begin{array}{lll} \textbf{line} & \lambda_1, \lambda_2 < 0 & |\lambda_1| \text{ and } |\lambda_2| >> |\lambda_3| \quad (3) \\ \textbf{plane} & \lambda_1 < 0 & |\lambda_1| >> |\lambda_2| \text{ and } |\lambda_3| \end{array}$$

For vessels, the eigenvector $\overrightarrow{v_3}$ associated with λ_3 will give the direction of the axis whereas $\overrightarrow{v_1}$ and $\overrightarrow{v_2}$ will give a basis in the plane orthogonal to the axis, as we shall prove later on a theoretical model.

4 Our method

Our approach is an extension of [KGSD95] and [LCBF97]. It can be split into three steps. We first compute the multiscale response $R_{multi}(I_0)$, then we extract the local extrema R^e_{multi} in $R_{multi}(I_0)$ and finally we create a skeleton of R^e_{multi} and visualize the results. In the first step, we use a model of the vessels both for interpreting the eigenvalues and the eigenvectors of the Hessian and for choosing a good normalization parameter.

4.1 Choice of an initial model

The first vessel model that we introduce is cylindrical with the z axis as the axis of the vessel and the section of the vessel being a Gaussian function:

$$I_0(x, y, z) = C\, G_{\sigma_0}(x, y) = \frac{C}{2\pi{\sigma_0}^2} e^{-\frac{x^2+y^2}{2{\sigma_0}^2}}.$$

where C is a constant and $\frac{C}{2\pi{\sigma_0}^2}$ represents the intensity at the center of the vessel (fig. 3) (C depends on the size and the location of the vessel). Properties of the model:

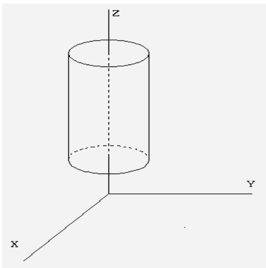

Figure 3: Initial model of a vessel.

- the frontier of the vessel is considered to be at points where the derivative of the intensity in the gradient direction is maximum, i.e. for the points which verify $x^2 + y^2 = {\sigma_0}^2$, so the radius of the vessel is σ_0.
- if the model is convolved with a Gaussian kernel of standard deviation s, the resulting image is another vessel which matches our model but with a different radius. This result can be directly deduced from the semi-group property.

4.2 Computation of the multiscale response

4.2.1 Multiscale response

We compute the multiscale response as the maximum of a set of responses taken at different scales, see equation (1). The scales are discretized from s_l to s_h using a logarithmic scale in order to have more precision at low scales where the standard deviation is smaller and where we want to detect smaller structures.

4.2.2 Pre-selection of candidates using the eigenvalues of the Hessian matrix

In order to compute the response at one scale $R_s(I_0)$, we need a pre-selection of the points that are near the axis of a vessel, and also a good estimation of the vectors $\overrightarrow{v_1}$ and $\overrightarrow{v_2}$ which give an orthogonal basis in the plane of a section. [LCBF97] already noticed (equation (3)) that a first criterion to detect line-like structures can be defined using the eigenvalues of the Hessian matrix. A formal derivation of our model allows us to check this criterion. The Hessian matrix can be expressed as $H = \frac{I_0}{{\sigma_0}^4} H_0$ where

$$H_0 = \begin{bmatrix} x^2 - {\sigma_0}^2 & xy & 0 \\ xy & y^2 - {\sigma_0}^2 & 0 \\ 0 & 0 & 0 \end{bmatrix}$$

and the eigenvalues of H_0 are

$$\begin{array}{lll} \lambda_3 = 0 & \lambda_2 = x^2 + y^2 - {\sigma_0}^2 & \lambda_1 = -{\sigma_0}^2 \\ \overrightarrow{v_3} = (0,0,1) & \overrightarrow{v_2} = (x,y,0) & \overrightarrow{v_1} = (-y,x,0) \end{array}$$

This result leads to the following conclusions for the model:

- Inside the vessel ($x^2 + y^2 < {\sigma_0}^2$) we have two negative eigenvalues with eigenvectors in the plane orthogonal to the axis of the vessel.
- The third eigenvalue is zero and the eigenvector associated is in the direction of the axis.
- the eigenvalues λ_1 and λ_2 are maximum in absolute value when $x = y = 0$ and are equal to $-\frac{I(x=0,y=0)}{{\sigma_0}^2}$.

In the case of a toric model, we have computed the eigenvalues and the eigenvectors and the results are similar except that the third eigenvalue is not null everywhere but only at the center of the vessel. It shows that a small curvature of the vessel doesn't change the previous conclusions. For the multiscale process, the model is convolved with a Gaussian kernel of standard deviation σ and the results are still valid due to the semi-group property but σ_0 has to be replaced by $\sqrt{\sigma_0^2 + \sigma^2}$. In conclusion, the relations of (3) can be replaced by (4) which are more restrictive but σ_0 is unknown and the criteria remain qualitative.

$$\frac{-\lambda_1({\sigma_0}^2 + \sigma^2)}{G_\sigma * I_0} \approx 1 \text{ and } \quad \lambda_1/\lambda_2 \approx 1 \text{ and } \quad \lambda_1 \gg \lambda_3 \quad (4)$$

4.2.3 Computation of the response R_s at one scale s

A first choice for R_s can be given by equation (2) as in [KGSD95]. An advantage of this choice is to ensure that a high response means that each of the four selected points has a high gradient and the probability of being at a vessel's center is high. Unfortunately, we noticed that in practice this criterion is not very robust to noise, and is easily defeated when two vessels are tangent to each other.

In order to increase the robustness of the method, we propose instead to use the integral response:

$$R_\sigma(x) = \frac{1}{2\pi\sigma} \int_{\alpha=0}^{2\pi} -\nabla_\sigma I(x + \sigma\overrightarrow{v_\alpha}).\overrightarrow{v_\alpha} d\alpha \quad (5)$$

with $\overrightarrow{v_\alpha} = cos(\alpha)\overrightarrow{v_1} + sin(\alpha)\overrightarrow{v_2}$. This integral is computed using $N = E(2\pi\sigma + 1)$ points along the circle $C(M, \sigma)$ of center $M(x)$ and of radius σ, where $E(x)$ is the integer part of x, it leads to the discrete formulation:

$$R_\sigma(x) = \frac{1}{N} \sum_{i=0}^{N-1} -\nabla_\sigma I(x + \sigma\overrightarrow{v_\alpha}).\overrightarrow{v_\alpha} \quad (6)$$

with $\alpha = 2\pi i/N$.

4.2.4 Normalization

One difficulty with multiscale approach is that we want to compare the result of a response function at different scales while the intensity and its derivatives are decreasing functions of scale.
Lindeberg [Lin94, Lin96] introduced the notion of normalized derivatives in order to deal with this problem. If the scale t is defined as $t = s^2 = \sigma^2$ where σ is the standard deviation of the Gaussian, the $\gamma-$ **normalized derivative** ∂_γ is defined as

$$\frac{\partial_\gamma(I * g_t)}{\partial x} = t^{\frac{\gamma}{2}} \frac{\partial(I * g_t)}{\partial x}$$

where $g_t = G_{\sqrt{t}} = G_\sigma = G_s$. The value of γ is chosen to allow the response $R_t(I_0)$ to be maximum for a scale corresponding to the size of the structure we want to detect. In practice, we need a model of the structure in order to estimate the value of γ. We usually take a model of the image as a defined function $I_0(M)$, then we decide which points we want to detect (for example the edges) and calculate their positions $P \subset \mathbb{R}^n$ in the image $I_t(M)$ at a scale t. Finally, we calculate the value of the scale $t_{max}(\gamma)$ which gives a maximum for the response function $R_t(I_0)$ at the points $M \in P$. Then we choose the value of γ that gives $t_{max}(\gamma) = s$ where s is the size of the structure. For instance, for edge detection purpose, Lindeberg [Lin96] obtained for a Gaussian blob the value $\gamma = \frac{3}{2}$. At a scale t, our model with a constant $C = 1$ leads to $L(x, y, z) = I_t(x, y, z) = I_0 * g_t = g_{t_0+t}$. We want to detect the vessel axis which is defined by $x = y = 0$. The response at a point $M(0,0,z)$ is given by:

$$R(I_0, t) = \frac{1}{2\pi\sqrt{t}} \int_{M \in C_{\sqrt{t}}} |\nabla L(x, y, t)(M).\vec{n}|$$

which corresponds to the mean of the vector product of the gradient with the unit radial vector along the circle of center M(0,0,z) and of radius $\sqrt{t} = \sigma$. The gradient and the normal vector $\vec{n}$ have the following expressions:

$$\begin{aligned} \nabla L(x, y, t) &= L(x, y, t) \frac{-1}{t + t_0} \begin{pmatrix} x \\ y \end{pmatrix} \\ \vec{n} &= \frac{1}{\sqrt{x^2 + y^2}} \begin{pmatrix} x \\ y \end{pmatrix} \\ \text{with} \quad & x^2 + y^2 = t \\ \text{so} \quad & \\ |\nabla L(x, y, t)(M).\vec{n}| &= \frac{\sqrt{t}}{2\pi\,(t + t_0)^2}\, e^{-\frac{t}{2(t+t_0)}} \end{aligned}$$

This last expression is no longer a function of M, so the mean of this expression along the circle is straightforward.

$$R = \frac{\sqrt{t}}{2\pi\,(t + t_0)^2}\, e^{-\frac{t}{2(t+t_0)}}.$$

The normalized response R_N is defined by $R_N = t^{\gamma/2} R$ and its partial derivative on t is:

$$\frac{\partial R_N}{\partial t} = \frac{t^{\frac{\gamma-1}{2}}}{4\pi\,(t + t_0)^4} e^{-\frac{t}{2(t+t_0)}} A$$

with

$$A = (\gamma - 3)t^2 + (2\gamma - 3)\, t_0\, t + (1 + \gamma)t_0^2$$

We are looking for the value of γ which gives a maximum for the function $R_N(t)$ at $t = t_0$. Thus we want $\frac{\partial R_N}{\partial t}$ to have a positive root which corresponds to a maximum. This leads to the necessary condition $\gamma < 3$. The sign of $\frac{\partial R_N}{\partial t}$ is then the same as $A = (\gamma-3)(t-t_1)(t-t_2)$, with $t_1 = \frac{2\gamma-3+\sqrt{21-4\gamma}}{2(3-\gamma)} t_0 > 0$ and $t_2 = \frac{2\gamma-3-\sqrt{21-4\gamma}}{2(3-\gamma)} t_0 < 0$ The maximum response is reached for $t_{max} = h(\gamma)t_0$ with $\gamma \in [0, 3[$. As we want $t_{max} = t_0$ (which is equivalent to $s_{max} = s_0$), γ must verify $h(\gamma) = 1$ which leads to $\gamma = \frac{5}{4}$ (Fig. 4).

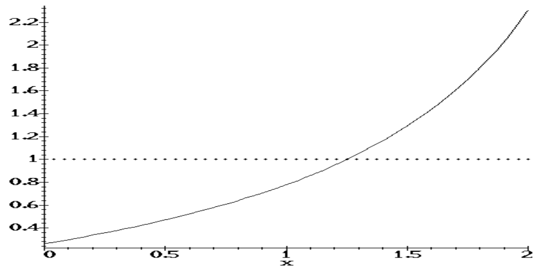

Figure 4: Representation of the function $h(\gamma)$ which shows the evolution of the scale which gives a maximum response: $t_{max} = h(\gamma)t_0$

4.3 Extraction of local extrema in $R_{multi}(I_0)$

For $M \in R_{multi}(I_0)$, we denote the scale at which M has been extracted as s and the eigenvectors at M and for the scale s as $\overrightarrow{v_1^s}$ and $\overrightarrow{v_2^s}$. From the image of the maximum of responses across the scales $R_{multi}(I_0)$ we create a new image where we keep only the points which are local extrema in the directions of $\overrightarrow{v_1^s}$ and $\overrightarrow{v_2^s}$ (equation. (7)).

$$\begin{aligned} R_{multi}(M) &\geq R_{multi}(M + \overrightarrow{v}) \\ &\text{with } \overrightarrow{v} \in \{\pm\overrightarrow{v_1^s}, \pm\overrightarrow{v_2^s}\}. \end{aligned} \tag{7}$$

4.4 Skeletonization and visualization

It is not an easy task to visualize the local extrema image in order to improve the interpretation of the original data image. For that purpose, we propose to extract some information of the local extrema image and to superimpose it into some 3D representation of the original data image (volume or surface rendering). *First*, we binarize the local extrema image by applying a hysteresis thresholding, with manually chosen thresholds. *Second*, we thin this result to obtain a skeleton-like representation of the vessels. Thinning is achieved by deleting the simple points. These points are the ones whose removal does not change the topology of the image. More details of the skeletonization algorithm can be found in [BM94]. The resulting skeleton is composed of pieces of curves, each of them representing a piece of vessel. *Third*, the skeleton is simplified by removing small pieces of curves. *Fourth*, the remaining curves are smoothed to better represent the vessel centerlines [Del94]. *Finally*, the results are visualized using the superimposition of an isosurface of the initial image with transparency and the skeleton which represents the center-lines of the vessels. A simple isosurface with a low threshold contains the small vessels but they are hidden by the big vessels. With a high threshold, the isosurface contains only the thickest vessels. This visualization allow us to check if the filtering gives a good result by combining the axis of all the vessels present in the image and by comparing with different isosurfaces.

5 Results

We have tested our algorithm on ten images $128 \times 128 \times 128$ ranging from easy to complex ones. The parameters s_l and s_h must be chosen according to the radius of the thinnest and the thickest vessels in the initial image. The algorithm was run with eight scales ranging from 0.5 to 4. The results on four different images are shown in Fig 5. The following interesting points are emphasized: most of the junction are detected without any discontinuity, tangent vessels are detected separately, some vessels with small radius and low intensity which are difficult to visualize in MIPs are well detected. A few illustrations of these properties are designated in the images by the letters J (Junction), T (Tangency), E (Enhancement) and L (Loop).

The detected centerlines combined with an isosurface using transparency are rotated in 3D, Movies 1 to 4 show this animation on the four images of Fig 5.

6 Conclusion and future work

We introduced a model of 3D vessels which allows us to choose several parameters of the multiscale detection. Our results are very promising and show that the algorithm has a good behavior on junctions and tangent vessels. Information obtained at the end of the filtering is more complex than the central line and should allow us to reconstruct the whole vessels. Another challenge is to detect automatically the presence of an aneurysm and to segment it, this will be the purpose of our future work.

References

[BM94] G. Bertrand and G. Malandain. A new characterization of three-dimensional simple points. *Pattern Recognition Letters*, 15(2):169–175, February 1994.

[Can86] J. Canny. A computational approach to edge detection. *IEEE Trans on Pattern Analysis and Machine Intelligence*, PAMI-8:679–698, November 1986.

[Del94] H. Delingette. Intrinsic stabilizers of planar curves. In *3rd European Conference on Computer Vision (ECCV'94)*, Stockholm, Sweden, June 1994.

[FKMP97] J.D. Furst, R.S. Keller, J.E. Miller, and S.M. Pizer. Image loci are ridges in geometric spaces. In *First Intern Conf on Scale-Space Theory in Computer Vision*, Utrecht, July 1997.

[KGSD95] T.M. Koller, G. Gerig, G. Székely, and D. Dettwiler. Multiscale detection of curvilinear structures in 2d and 3d image data. In *Fifth International Conference on Computer Vision*, pages 864–869, Cambridge USA, June 1995.

[LCBF97] C. Lorenz, I.-C. Carsen, T.M. Buzug, C. Fassnacht, and J. Weese. Multi-scale line segmentation with automatic estimation of width, contrast and tangential direction in 2d and 3d medical images. In *CVRMed-MRCAS'97*, pages 213–222, Grenoble, France, March 1997. Lecture notes in Computer Science 1205, Springer Verlag.

[Lin94] T. Lindeberg. *Scale-Space Theory in Computer Vision*. Kluwer Academic Publishers, Dordrecht, Netherlands, 1994.

[Lin96] T. Lindeberg. Edge detection and ridge detection with automatic scale selection. In *IEEE Comp. Soc. Conf. on Computer Vision and Pattern Recognition*, page 465, San Francisco, June 1996.

[Pay96] Etienne Payot. *Reconstruction Vasculaire tridimensionnelle en imagerie par rayons X*. Ph.D. dissertation, Ecole Nationale Supérieure des Télécommunication, 1996.

[SNAK97] Y. Sato, S. Nakajima, H. Atsumi, T. Koller, G. Gerig, S. Yoshida, and R. Kikinis. 3d multi-scale line filter for segmentation and visualization of curvilinear structures in medical images. In *CVRMed-MRCAS'97*, pages 213–222, March 1997. Lecture Notes in Computer Science 1205, Springer Verlag.

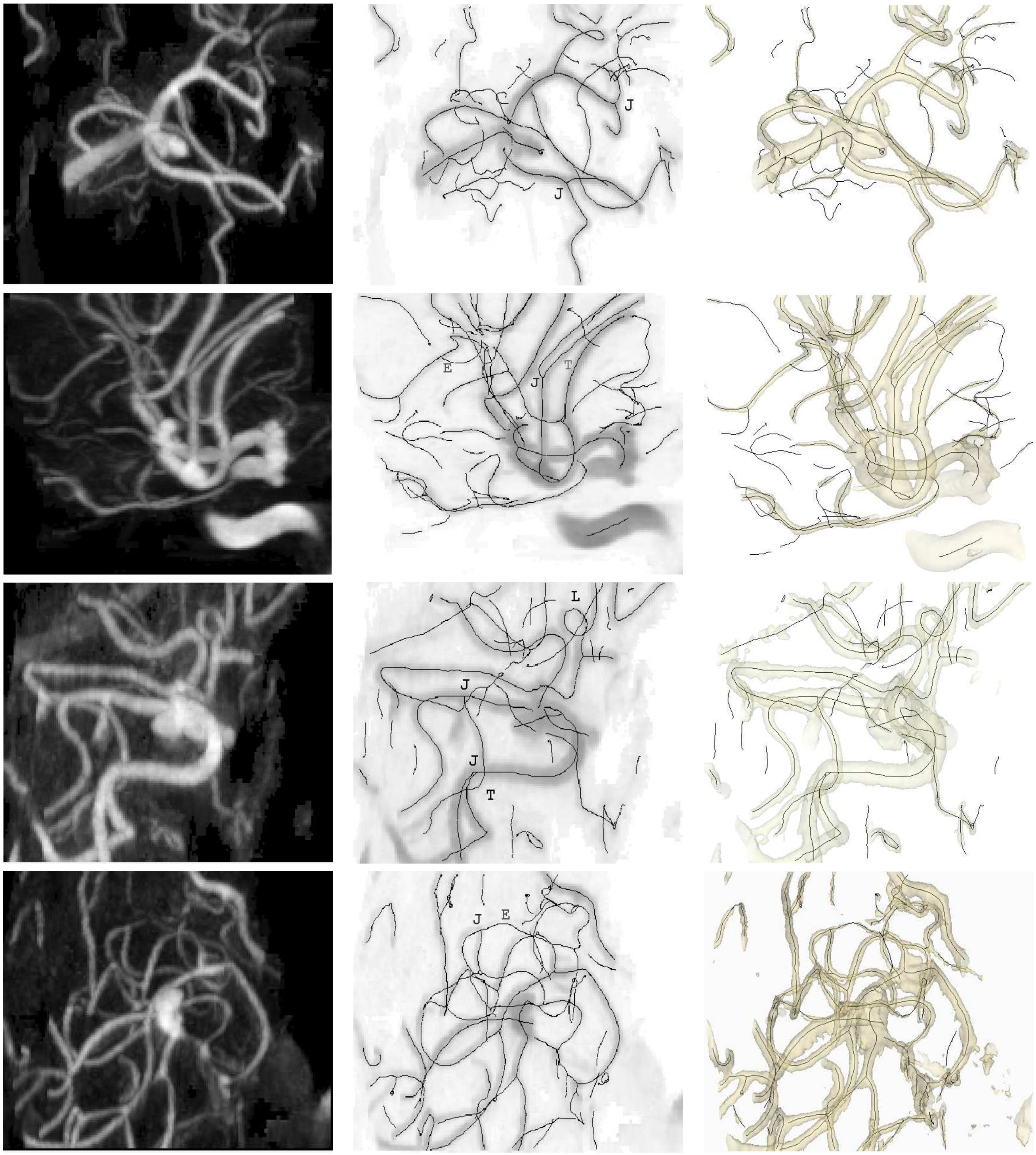

Figure 5: **From top to bottom,** the results of the 3D vessels detection on four images, using a fixed point of view. **From left to right,** Maximum Intensity Projection of the initial image, the detected centerlines superimposed on a Maximum Intensity Projection using a white background, the detected centerlines combined with an isosurface using transparency .